A Peripheral Benzodiazepine Receptor Targeted Agent for In Vitro Imaging and Screening

ARTICLE *in* BIOCONJUGATE CHEMISTRY · MAY 2006

Impact Factor: 4.51 · DOI: 10.1021/bc060020b · Source: PubMed

8 AUTHORS, INCLUDING:

Michelle Sexton
Center for the Study of Cannabis and Social …
11 PUBLICATIONS **90** CITATIONS
SEE PROFILE

Mingfeng Bai
University of Pittsburgh
40 PUBLICATIONS **282** CITATIONS
SEE PROFILE

Kristin Cederquist
IMRA America, Inc.
12 PUBLICATIONS **346** CITATIONS
SEE PROFILE

Darryl J Bornhop
Vanderbilt University
130 PUBLICATIONS **2,304** CITATIONS
SEE PROFILE

A Peripheral Benzodiazepine Receptor Targeted Agent for In Vitro Imaging and Screening

H. Charles Manning,[†,‡] Sarah M. Smith,[†] Michelle Sexton,[†,§,||] Sarah Haviland,[†] Mingfeng Bai,[†] Kristin Cederquist,[†] Nephi Stella,[§] and Darryl J. Bornhop*[,†]

Department of Chemistry, Vanderbilt University, Nashville, Tennessee 37235, Vanderbilt University Institute of Imaging Science and Department of Radiology and Radiological Sciences, Nashville, Tennessee 37235, Department of Pharmacology, Psychiatry, and Behavioral Science, University of Washington, Seattle, Washington 98195, and Department of Basic Sciences, School of Naturopathic Medicine, Bastyr University, Seattle, Washington 98028. Received January 26, 2006; Revised Manuscript Received March 24, 2006

We developed a molecular imaging agent (MIA), a conjugable form of PK11195 (conPK11195) coupled to a lissamine dye (Liss−ConPK11195), which targets the peripheral benzodiazepine receptor (PBR). To determine that our compound specifically binds to this 18 kDa protein, primarily expressed on the mitochondria, we performed classic binding studies on live MDA-MB-231 breast cancer cells and measured fluorescence in cell fractions of C6 glioma cells. We found that conPK11195 conjugated to the fluorophore retained significant binding to its target. Here we demonstrate the utility of the agent for in vitro imaging of live cells by specific binding to the protein of interest.

INTRODUCTION

Molecular imaging (MI) has the potential to revolutionize biological investigations and diagnostic medicine. For example, discrete intracellular molecular events can be followed in vitro in real time (*1*, *2*), and MI agents allow the in vivo study of disease progression and therapeutic efficacy monitoring (*3*−*5*). Numerous ligands have been functionalized for nuclear imaging such as autoradiography (*6*) and positron emission tomography (PET) (*7*), yet synthetic complexity, short half-life of radioligands, and expense of the detection methodologies are limitations to these applications of molecular imaging. Immunohistochemistry continues to be a valuable tool for cellular scale imaging in vitro, but the numerous steps involved in this technique make this a somewhat tedious process. The development of targeted imaging agents for in vitro screening of protein expression as well as in vitro therapy efficacy monitoring is an emerging concept in MI. Fluorescent agents with high specificity and attractive spectroscopic properties are therefore needed in the biomedical research community.

The peripheral benzodiazepine receptor (PBR), reported to be expressed primarily by mitochondria (*8*, *9*), is known to be associated with numerous biological functions including regulation of cellular proliferation, immunomodulation, regulation of cholesterol transport and steroidogenesis, and apoptosis (*10*). The precise biological relevance and clinical significance of PBR in disease progression has remained somewhat elusive, yet the overexpression in cancer (*11*, *12*) and neurodegenerative disease (*13*−*15*) is well-documented as is its correlation with metastasis and poor clinical prognosis (*16*−*18*).

Several exogenous PBR ligands have been developed which bind PBR with high affinity, including PK11195 (*19*), DAA1106 (*20*, *21*), and Ro5-4864 (*22*). Both ^{3}H- and ^{11}C-PK11195 have been used for human imaging of glioma (*23*−*26*), neurodegenerative disease (*27*), and stroke (*28*).

Papadopolous et al. reported an agent for in vitro analysis, NBD-FGIN 1-27, utilizing a fluorophore (NBD) that is not optimal for in vitro imaging (*29*). With the principal excitation and emission wavelengths for NBD (7-nitro-2,1,3-benzoxadiazole) at 466 nm and 536 nm, respectively (*30*), the effective signal-to-noise ratio for detection in cells and tissues tends to be limited by autofluorescence and scatter, especially when compared to longer wavelength dyes (*1*). Furthermore, the fluorescence sensitivity of NBD agents is limited by relatively low ($\sim$8000 L mol^{-1} cm^{-1}) aqueous phase molar extinction coefficients (*30*). More recently, Chen et al has prepared PBR targeted photodynamic therapy (PDT) probes based on pyropheophorbide metal complexes (*31*). These probes appear to have utility for therapeutic purposes, but the potential for performing imaging with these compounds is less clearly defined (*31*).

We recently reported another PBR targeted MI agent, a lanthanide chelate (Ln-PK11195) (*32*, *33*). This agent is unique because it has the potential to provide both an optical and MR signature depending on the metal ion that is chelated (i.e. Eu^{3+} for optical and Gd^{3+} for MR) (*34*). While we demonstrated optical microscopy of live cells using the europium chelate (*34*), excitation of the sensitizing antenna at 320 nm is unattractive due to the high energy of UV radiation, and the attenuated transmission through glass optical trains of standard microscopes limits the usefulness of this agent.

To address this limitation, we have prepared Liss−ConPK11195, which has a relatively high molar extinction coefficient, thus allowing improved sensitivity for microscopy imaging and high-throughput screening detection in multiwell plates. Here we report the synthesis and spectroscopic characterization of Liss−ConPK11195, demonstrate specific binding in live cells, and confirm the intracellular location by isolation of the mitochondrial fraction.

EXPERIMENTAL PROCEDURES

Synthesis and Spectroscopic Characterization of Liss−ConPK11195. Lissamine−Rhodamine B sulfonyl chloride was

* Corresponding author. Mailing address: Vanderbilt University, 7300 Stevenson Center, Nashville, TN 37235. Tel: 615.322.4226. Fax: 615.343.1234. E-mail: Darryl.Bornhop@Vanderbilt.Edu.

[†] Department of Chemistry, Vanderbilt University.

[‡] Vanderbilt University Institute of Imaging Science and Department of Radiology and Radiological Sciences.

[§] University of Washington.

[||] Bastyr University.

10.1021/bc060020b CCC: $33.50
Published on Web 05/03/2006

purchased from Molecular Probes. Conjugable PK11195 (as previously reported (*33*)) was dissolved in dry chloroform along with 1 equiv of triethylamine (TEA). Next, 1.5 equiv of Lissamine−Rhodamine B sulfonyl chloride was added in one part. The vessel was purged with argon, and the reaction was allowed to continue overnight. Formation of the product was monitored via thin-layer chromatography (TLC) ($R_f = 0.8$, 9:1 chloroform/methanol). Purification of the product was achieved using column chromatography on silica, eluting with a 30:1:0.1 mixture of chloroform, methanol, and aqueous ammonia. Absorbance was measured using a Shimadzu 1700 spectrophotometer, and fluorescence was recorded using a PTI fluorometer.

^{1}H NMR ($CDCl_3$): δ 1.31 (t, 12H), 1.42 (m, 2H), 1.54 (m, 2H), 1.67 (bs, 4H), 2.90 (q, 2H), 3.39 (m, 2H), 3.57 (q, 8H), 6.70 (d, 2H), 6.87 (d, 2H), 7.20 (m, 3H), 7.46−7.57 (m, 6H), 7.65 (m, 1H), 7.73 (m, 1H), 8.03 (d, 1H), 8.22 (t, 1H), 8.36 (d, 1H), 8.63 (s, 1H), 8.73 (s, 1H).

ESI MS+ (calcd: found): (921.32: 922.45 and 944.44 M + Na^+).

Tissue Culture. C6 glioma cells were cultured in Dulbecco's modified Eagle medium (DMEM)−F12 medium (Gibco/Invitrogen) supplemented with 0.1% gentamicin sulfate (Biowhittaker). Standard medium pH was adjusted to 7.4. Cells were maintained in a tissue culture incubator (Forma Scientific) at 37 °C, 5% CO_2. MDA-MB-231 cells were cultured in closed cap flasks, with 90% Leibovitz's L-15 medium, supplemented with 2 mM L-glutamine and 10% fetal bovine serum.

PBR Binding Affinity Determinations. A standard fluorescence calibration curve for Liss−ConPK11195 was prepared using a Beckman Coulter DTX 880 plate reader and found linear over the concentration range 0−10 μM. Twenty-four hours prior to performing the binding experiments, MDA-MB-231 cells were plated into NUNC 96 well (optical) plates at a density of 4×10^4 cells (80% confluence). To measure specific binding, cells were incubated in triplicate for 30 min with standard dilutions of Liss−ConPK11195 (0, 1 μM, 3.2 μM, 10 μM, 32 μM) without and with excess (10 μM "cold") unlabeled DAA1106 (prepared as previously reported) (*35*). The plate was subsequently rinsed with MEM/Cellgro and read on the plate reader. When the values for the nonspecific binding were subtracted from the total, the specific binding signal was revealed. These data were analyzed by Scatchard analysis using Graphpad Prism software.

Live Cell Imaging. Cells were plated in MaTek dishes and incubated with the imaging agent by first aspirating the growth media and then adding media containing the contrast agent. Incubation concentrations ranged from 1 nM to 100 μM, although concentrations above 10 μM seemed to produce nonspecific staining in the microscopy experiments (data not shown). The cells were incubated with the imaging agent for 45 min at 37 °C, 5% CO_2 as previously reported (*29*). At the end of the incubation time, cells were rinsed with fresh medium three times and imaged.

PBR Functional Displacement of Liss−ConPK11195. Forty-eight hours prior to imaging, 2.5×10^4 C6 glioma cells were plated into MaTek dishes and propagated at 37 °C under 5% CO_2. The cells were either incubated for 45 min with 1 μM Liss−ConPK11195 or coincubated for 45 min with 1 μM Liss−ConPK11195 and 100 μM PK11195 (Sigma-Aldrich). The cells were subsequently rinsed with saline to remove any unbound contrast agent, and then imaged using fluorescence microscopy. The cellular fluorescence intensity was evaluated by measuring the gray scale intensities of individual cells from multiple assays. A one-way ANOVA (Prism 4.0) at the 95% confidence level was used to indicate the statistical significance of the data.

Microscopy. Microscopy was performed using a Nikon TE 2000-U inverted microscope, coupled to a Q-Imaging RetigaEXi camera. Image acquisition was controlled using Metamorph (version 6.2). The optical train used to image Liss−ConPK11195 consisted of a mercury lamp and a Texas Red filter set (Chroma, excitation 575 nm × 20 nm, emission 625 nm × 50 nm). Confocal microscopy was performed using a Zeiss LSM510 confocal microscope, 543 nm excitation line and emission collected through a 620 nm × 50 nm filter.

Mitochondrial Fractionation Assay. Cellular Disruption. A total of ninety (90) 10 cm culture flasks of C6 glial cells were propagated to near confluency. Half of the plates (45) were incubated with 1 μM Liss−ConPK11195 for 45 min, and the other half (45) were left unincubated as control. At the end of the incubation time, each plate of cells was rinsed with approximately 5 mL of ice-cold disruption buffer ("H" buffer, 5 mM HEPES, 0.21 M D-mannitol, 0.07 M sucrose, 2 mM benzamidine, 2 mM α-toluenesulfonyl fluoride, 4 mM magnesium chloride, pH 7.4) (5×), and then the monolayer was scraped from the surface of the dish. The combined scrapings from the labeled and unlabeled plates were separately resuspended in ice-cold disruption buffer to yield 10 mL total volume. The cells were then ruptured by 50 strokes with a glass homogenizer, type A pestle. The homogenates were centrifuged at 200*g* for 1 min. The resulting pellet was then rehomogenized in ice-cold disruption buffer (diluted to 1/4 strength) and centrifuged at 200*g* for 1 min. Next, the supernatants were combined and centrifuged at 200*g* for 1 min. The resulting supernatant was filtered through four layers of cheesecloth and centrifuged at 0.6K × *g* for 20 min (fraction 1). The resulting supernatant was then centrifuged at 10K × *g* for 2 h, and the pellet (fraction 2) was separated from the supernatant (fraction 3).

Mitochondrial Fluorescence Assay. Fluorescence measurements were made using a PTI fluorimeter and standard quartz cuvettes. A fluorescence calibration curve was prepared using increasing concentrations of Liss−ConPK11195 solution in PBS (1−20 nm). Samples (1.5 mg/mL) from fractions 1 and 2 were prepared by diluting the pellet 100:1 in PBS. Fraction 3 was run neat. Samples were excited at 571 nm, and the emission was scanned from 580 nm to 630 nm. The principal emission band was found at 585 nm, and the reported fluorescence values are from said wavelength.

Corrected Mitochondrial Activity. Succinate dehydrogenase activity was assayed via the colorimetric reduction of iodonitrotetrazolium (INT) chloride using a protocol previously reported (*36*). Briefly, to prepare the enzyme solution, a 20 μL protein suspension (1.5 mg/mL verified by the Bradford assay) was added to 500 μL of freshly prepared INT reagent (~35 °C) and absorbance was continuously monitored at 500 nm for 10 min (triplicate measurement). The INT reagent without succinate, subtracted from the sample rates, served as a control. The specific activity was calculated according to the following equation: units/mL = ΔA/min × 5.18. A one-way ANOVA (Prism 4.0) at the 95% confidence level was used to indicate the statistical significance of the data. INT reagent = 100 mM triethanolamine, 0.5 mM EDTA, 2 mM INT, 12 g/L Tween 20, 20 mM succinic acid.

RESULTS AND DISCUSSION

We synthesized a PBR targeted MI agent, Liss−ConPK11195, by labeling our previously reported conjugable PK11195 ligand (*33*) with Lissamine−Rhodamine B sulfonyl chloride (Scheme 1). The agent was easily purified using standard column chromatography on silica gel. To determine whether the structure/function relationship of the dye was changed upon coupling, we measured the absorbance and fluorescence properties of Liss−ConPK11195 in aqueous media (Figure 1). The absorption maximum was centered at 571 nm, and emission was centered at 585 nm, similar to that of the

Scheme 1. Synthesis of Liss−ConPk11195

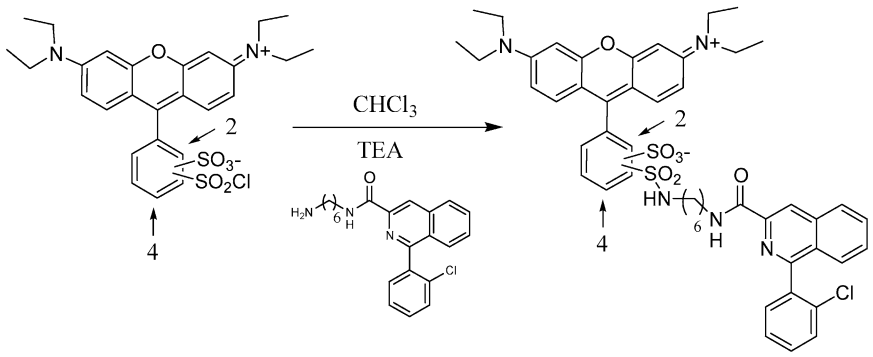

free dye. The molar extinction coefficient for Liss−ConPK11195 was determined to be 35 000 L mol^{-1} cm^{-1} in water, enabling sensitive detection of the imaging agent and demonstrating that conjugation did not significantly alter the function of the dye. While the absorbance and emission bands for Liss−ConPK11195 do not show as large a Stokes shift as the previously reported lanthanide chelate agent−PBR agent (*33*), it does have spectral characteristics leading to utility for fluorescence microscopy and commercially available fluorescence plate readers.

We next determined that conjugation of the dye to the ligand did not prevent binding to the target and that it was specific for PBR. We performed a classic binding assay in a multiwell plate in a live-cell format. Binding affinity (K_d) of Liss−ConPK11195 to PBR was calculated to be 1 μM (data not shown). While this value is higher than expected for an unperturbed PK11195 analogue, the imaging work shown here and by others (*31*) demonstrates that PBR targeted agents with micromolar binding affinities still have utility for cellular targeting applications. It is likely that the presence of the bulky, charged fluorophore and the minor structural differences between PK11195 and the conjugable PK11195 analogue contribute to a reduced binding affinity (*33*).

Fluorescence microscopy was used to characterize the cellular uptake and distribution of Liss−ConPK11195 in PBR overexpressing C6 glioma and MDA-MB-231 breast cancer cells. We first incubated live C6 glioma cells with the imaging agent (10 μM) and then rinsed the cells and imaged them using an epi-illumination fluorescence microscope. As controls, we imaged a similar population of cells with Lissamine after incubation with the free dye (nontargeted, 10 μM) and another population of unincubated cells to evaluate the level of autofluorescence. As seen in Figure 2A−D, both controls (unlabeled (A, B) and free Lissamine labeled (C, D) C6 cells) lack fluorescence, while cells incubated with Liss−ConPK11195 (Figure 2E,F) show perinuclear fluorescence. Fluorescence was also easily detected by microscopy in C6 cells at a concentration of 100 nM (data not shown). MDA-MB-231 breast cancer cells were imaged identically with a 100 nM concentration Liss−ConPK11195 yielding bright perinuclear fluorescence (Figure 3). Controls were the same as with the C6 cells and are shown in Figure 3A−D.

Confocal microscopy verified that Liss−ConPK11195 was internalized in C6 cells labeled with the MI agent as previously described. Fluorescence appeared to be perinuclear while no fluorescence was visualized on the cell surface (Figure 4). These images are consistent with previous reports describing the

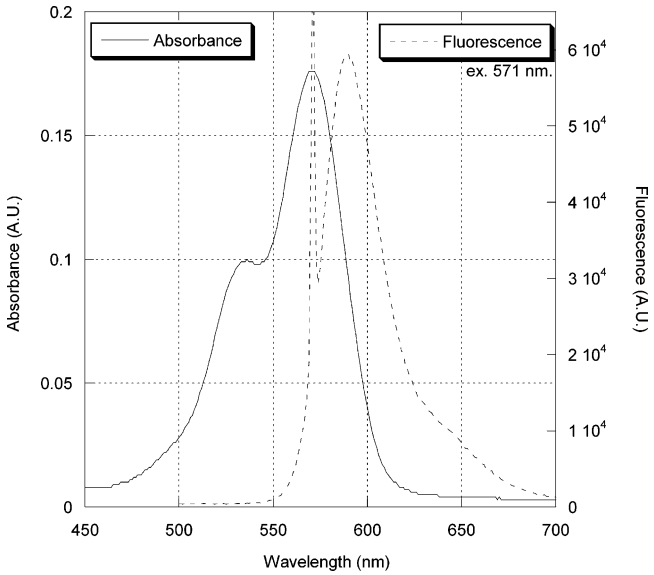

Figure 1. Liss−ConPK11195 aqueous spectroscopy (agent concentration = 5 μM).

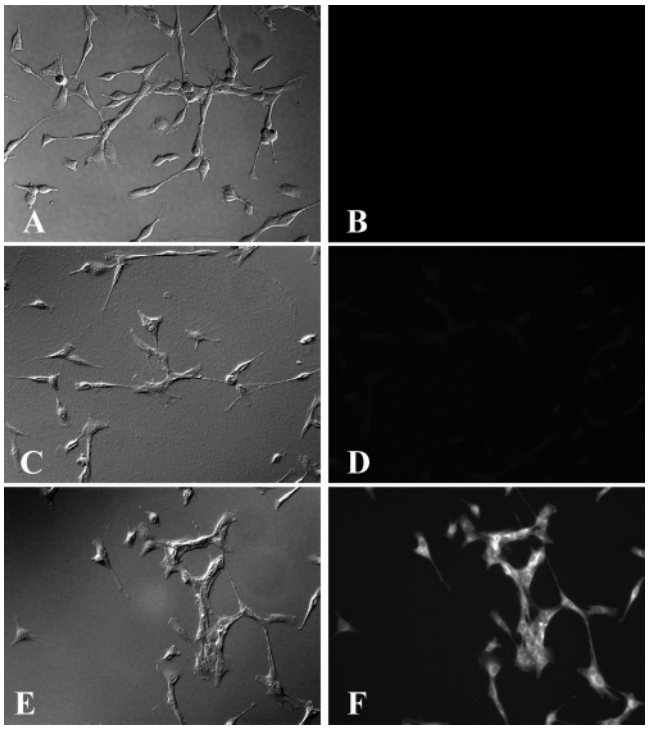

Figure 2. Fluorescent labeling studies of PBR in C6 glioma cells using Liss-PK11195. C6 cells were cultured on glass coverslips and incubated with either 10μM Lissamine free dye or Liss−ConPK11195 at 37 °C for 30 min. (A) Whitelight DIC image, unlabeled control. (B) Fluorescence image, unlabeled control. (C) Whitelight DIC image, cells incubated with 10 μM Lissamine free dye. (D) Fluorescence image, Lissamine control. (E) Whitelight DIC image, cells incubated with 10 μM Liss−ConPK11195. (F) Fluorescence image, cells incubated with Liss−ConPK11195.

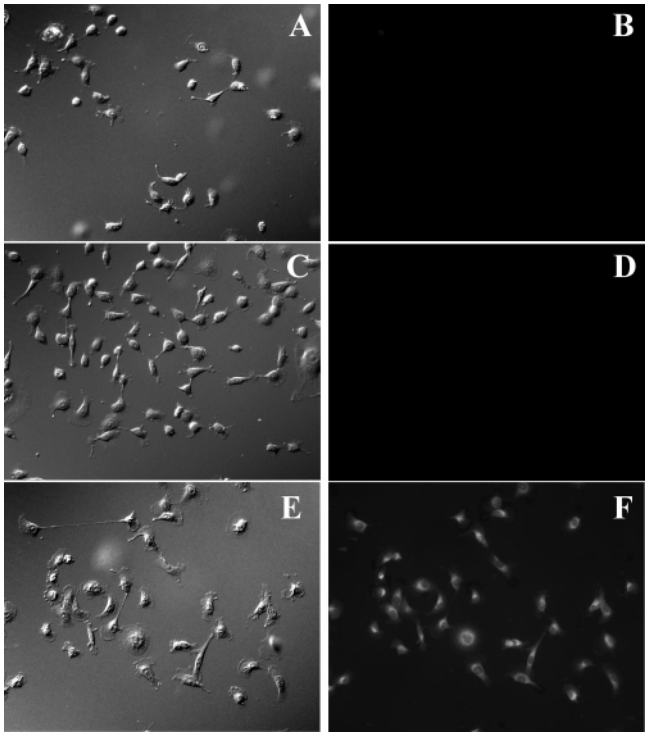

Figure 3. Fluorescent labeling studies of PBR in MDA-MB-231 cells using Liss−ConPK11195. MDA-MB-231 cells were cultured on glass coverslips and incubated with either 100 nM Lissamine free dye or Liss−ConPK11195 at 37 °C for 30 min. (A) Whitelight DIC image, unlabeled control. (B) Fluorescence image, unlabeled control. (C) Whitelight DIC image, cells incubated with 100 nM Lissamine free dye. (D) Fluorescence image, Lissamine control. (E) Whitelight DIC image, cells incubated with 100 nM Liss−ConPK11195. (F) Fluorescence image, cells incubated with Liss−ConPK11195.

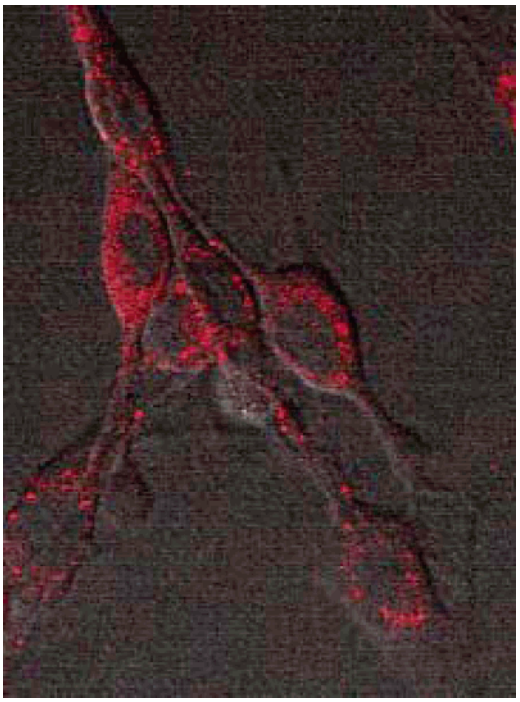

Figure 4. Confocal imaging of PBR in C6 rat glioma cell line. C6 cells were labeled with 1 μM Liss−ConPK11195 and imaged using a Zeiss confocal microscope. False color fluorescence image/DIC overlay demonstrating typical cellular morphology and predominately perinuclear fluorescence.

primary intracellular location of PBR and immuohistochemical PBR staining (*29*).

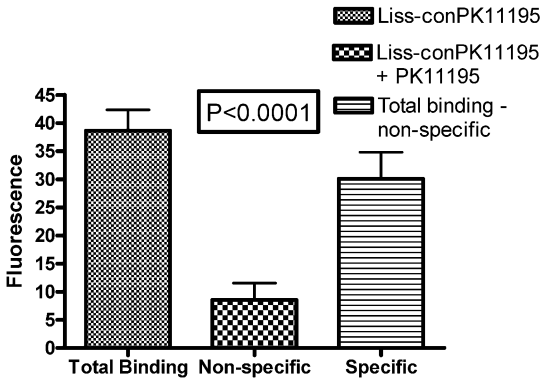

Figure 5. Live cell fluorescence displacement of 1 μM Liss−ConPK11195 with 100-fold excess PK 11195 in C6 glioma cells. Left bar: total binding. Middle bar: nonspecific binding. Right bar: specific binding. Autofluorescence was subtracted from each value. *P* value was calculated via one-way ANOVA, comparing fluorescence intensity of total, nonspecific, and specific binding.

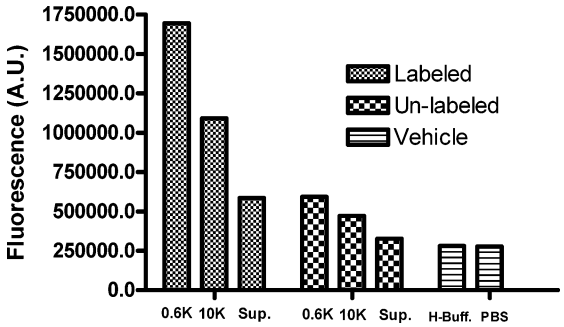

Figure 6. Fluorescence intensity from C6 cellular fractionations, 10K × *g*, 0.6K × *g*, and supernatant. Bars represent fluorescence intensity from labeled, unlabeled, and vehicle (control) samples.

An optical competitive binding assay was performed with live C6 glioma cells using excess "cold" PK11195 as the competitor with the dye. Labeled, unlabeled, and PK11195 challenged cells were imaged with fluorescence microscopy. Conservation of imaging settings, including integration time, binning, and magnification, gave a direct comparison of the cells labeled under the various medium conditions, and we quantified the displacement by subtracting the nonspecific binding from the total binding. Figure 5 shows total, specific, and nonspecific binding, with the statistical significance of all three measurements verified by one-way ANOVA analysis ($P < 0.0001$).

Cellular fractionation (*37*) confirmed the observations of the intracellular localization made by microscopy. A standard fluorimeter was used to measure fluorescence in mitochondrial and cytosolic cell fractions. C6 glioma cells were incubated with and without (control) Liss−ConPK11195, rinsed, and then mechanically disrupted. Lysates were then purified using a protocol that yields two mitochondrial-rich fractions (0.6K × *g* and 10K × *g*) (*37*). Next, we measured the relative fluorescence emission (excitation 571 nm, emission 580−630 nm) of all the cellular fractions collected (cytosol, 0.6K × *g* fraction, and 10K × *g* fraction). Liss−ConPK11195 fluorescence was detected in all three fractions with significant binding in the 0.6K × *g* and the 10K × *g* mitochondrial fractions (Figure 6). Fluorescence in the cytosolic fraction (supernatant) was detectable, yet miniscule in comparison to the other fractions measured, and suggests either nonspecific binding or binding to another protein in the cytosolic fraction. Fluorescence values for unlabeled cells and vehicle (as control) represent the bacK × ground signal and indicate some autofluorescence at the measured wavelength. Mitochondrial content of the assayed fractions was confirmed by measuring succinate dehydrogenase

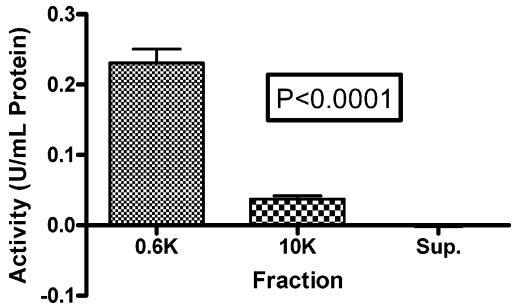

Figure 7. Corrected specific succinate dehydrogenase (mitochondrial) activity (U/mL) for the three assayed cellular fractions. Value represents the difference between the experimental and control (nonspecific) activities for each sample. *P* value calculated via one-way ANOVA.

activity (Figure 7). As expected, the mitochondrial fractions had statistically significant succinate dehydrogenase activity compared to the cytosolic fraction ($P < 0.0001$).

CONCLUSIONS

In this report we have demonstrated the synthesis, spectroscopic, and biological characterization of a novel optical molecular imaging agent targeting PBR. Liss−ConPK11195 specifically binds to PBR and displays attractive optical properties for live cell fluorescence microscopic imaging and high-throughput plate reader assays. While immunofluorescence has been a valuable technique for measuring proteins of interest in fixed cells, live cell molecular imaging has the potential to be translated to rapid high-throughput screening of therapies and to in vivo imaging. With molecular imaging being used increasingly in medical diagnostics, it is important to identify potential agents for reporting physiological processes such as protein expression. Here we show that simple synthetic chemistry can be used to enhance in vitro studies of disease processes, by targeting PBR expression with an optical imaging agent.

ACKNOWLEDGMENT

The authors would like to acknowledge Dr. Vassilios Papadopoulos for helpful discussions and assistance with the mitochondrial assay.

LITERATURE CITED

(1) Weissleder, R., and Mahmood, U. (2001) Molecular imaging. *Radiology 219*, 316−333.

(2) Gaietta, G., Deerinck, T. J., Adams, S. R., Bouwer, J., Tour, O., Laird, D. W., Sosinsky, G. E., Tsien, R. Y., and Ellisman, M. H. (2002) Multicolor and electron microscopic imaging of connexin trafficking. *Science 296*, 503−507.

(3) Tung, C. H., Mahmood, U., Bredow, S., and Weissleder, R. (2000) In vivo imaging of proteolytic enzyme activity using a novel molecular reporter. *Cancer Res. 60*, 4953−4958.

(4) McIntyre, J. O., and Matrisian, L. M. (2003) Molecular imaging of proteolytic activity in cancer. *J. Cell. Biochem. 90*, 1087−1097.

(5) Wu, J. C., Sundaresan, G., Iyer, M., and Gambhir, S. S. (2001) Noninvasive optical imaging of firefly luciferase reporter gene expression in skeletal muscles of living mice. *Mol. Ther. 4*, 297−306.

(6) Myers, R., Manjil, L. G., Cullen, B. M., Price, G. W., Frackowiak, R. S. J., and Cremer, J. E. (1991) Macrophage and Astrocyte Populations in Relation to [H-3] Pk 11195 Binding in Rat Cerebral-Cortex Following a Local Ischemic Lesion. *J. Cereb. Blood Flow Metab. 11*, 314−322.

(7) Maeda, J., Suhara, T., Zhang, M. R., Okauchi, T., Yasuno, F., Ikoma, Y., Inaji, M., Nagai, Y., Takano, A., Obayashi, S., and Suzuki, K. (2004) Novel peripheral benzodiazepine receptor ligand [C-11]DAA1106 for PET: An imaging tool for glial cells in the brain. *Synapse 52*, 283−291.

(8) Anholt, R. R. H., Pedersen, P. L., Desouza, E. B., and Snyder, S. H. (1986) The Peripheral-Type Benzodiazepine Receptor−Localization to the Mitochondrial Outer-Membrane. *J. Biol. Chem. 261*, 576−583.

(9) Basile, A. S., and Skolnick, P. (1986) Subcellular-Localization of Peripheral-Type Binding-Sites for Benzodiazepines in Rat-Brain. *J. Neurochem. 46*, 305−308.

(10) Casellas, P., Galiegue, S., and Basile, A. S. (2002) Peripheral benzodiazepine receptors and mitochondrial function. *Neurochem. Int. 40*, 475−486.

(11) Miettinen, H., Kononen, J., Haapasalo, H., Helen, P., Sallinen, P., Harjuntausta, T., Helin, H., and Alho, H. (1995) Expression of Peripheral-Type Benzodiazepine Receptor and Diazepam-Binding Inhibitor in Human Astrocytomas−Relationship to Cell-Proliferation. *Cancer Res. 55*, 2691−2695.

(12) Han, Z., Slack, R. S., Li, W., and Papadopoulos, V. (2003) Expression of peripheral benzodiazepine receptor (PBR) in human tumors: relationship to breast, colorectal, and prostate tumor progression. *J. Recept. Signal Transduction Res. 23*, 225−238.

(13) Messmer, K., and Reynolds, G. P. (1998) Increased peripheral benzodiazepine binding sites in the brain of patients with Huntington's disease. *Neurosci. Lett. 241*, 53−56.

(14) Rao, V. L. R., Dogan, A., Bowen, K. K., and Dempsey, R. J. (2000) Traumatic brain injury leads to increased expression of peripheral-type benzodiazepine receptors, neuronal death, and activation of astrocytes and microglia in rat thalamus. *Exp. Neurol. 161*, 102−114.

(15) Banati, R. B. (2002) Visualising microglial activation in vivo. *Glia 40*, 206−217.

(16) Hardwick, M., Fertikh, D., Culty, M., Li, H., Vidic, B., and Papadopoulos, V. (1999) Peripheral-type benzodiazepine receptor (PBR) in human breast cancer: Correlation of breast cancer cell aggressive phenotype with PBR expression, nuclear localization, and PBR-mediated cell proliferation and nuclear transport of cholesterol. *Cancer Res. 59*, 831−842.

(17) Hardwick, M., Rone, J., Han, Z. Q., Haddad, B., and Papadopoulos, V. (2001) Peripheral-type benzodiazepine receptor levels correlate with the ability of human breast cancer MDA-MB-231 cell line to grow in SCID mice. *Int. J. Cancer 94*, 322−327.

(18) Maaser, K., Grabowski, P., Sutter, A. P., Hopfner, M., Foss, H. D., Stein, H., Berger, G., Gavish, M., Zeitz, M., and Scherubl, H. (2002) Overexpression of the peripheral benzodiazepine receptor is a relevant prognostic factor in stage III colorectal cancer. *Clin. Cancer Res. 8*, 3205−3209.

(19) Benavides, J., Quarteronet, D., Imbault, F., Malgouris, C., Uzan, A., Renault, C., Dubroeucq, M. C., Gueremy, C., and Lefur, G. (1983) Labeling of Peripheral-Type Benzodiazepine Binding-Sites in the Rat-Brain by Using [Pk-H-3 11195, an Isoquinoline Carboxamide Derivative−Kinetic-Studies and Autoradiographic Localization. *J. Neurochem. 41*, 1744−1750.

(20) Chaki, S., Funakoshi, T., Yoshikawa, R., Okuyama, S., Okubo, T., Nakazato, A., Nagamine, M., and Tomisawa, K. (1999) Binding characteristics of [H-3]DAA1106, a novel and selective ligand for peripheral benzodiazepine receptors. *Eur. J. Pharmacol. 371*, 197−204.

(21) Culty, M., Silver, P., Nakazato, A., Gazouli, M., Li, H., Mura-matsu, M., Okuyama, S., and Papadopoulos, V. (2001) Peripheral benzodiazepine receptor binding properties and effects on steroid synthesis of two new phenoxyphenyl-acetamide derivatives, DAA1097 and DAA1106. *Drug Dev. Res. 52*, 475−484.

(22) File, S. E., and Pellow, S. (1983) Ro5-4864, a Ligand for Benzodiazepine Micromolar and Peripheral Binding-Sites−Antagonism and Enhancement of Behavioral-Effects. *Psychopharmacology 80*, 166−170.

(23) Starosta-Rubinstein, S., Ciliax, B., Penney, J., McKeever, P., and Young, A. (1987) Imaging of a glioma using peripheral benzodiazepine receptor ligands. *Proc. Natl. Acad. Sci. U.S.A. 84*, 891−895.

(24) Junck, L., Olson, J. M. M., Ciliax, B. J., Koeppe, R. A., Watkins, G. L., Jewett, D. M., Mckeever, P. E., Wieland, D. M., Kilbourn, M. R., Starostarubinstein, S., Mancini, W. R., Kuhl, D. E., Greenberg, H. S., and Young, A. B. (1989) Pet Imaging of Human Gliomas with Ligands for the Peripheral Benzodiazepine Binding-Site. *Ann. Neurol. 26*, 752−758.

(25) Pappata, S., Cornu, P., Samson, Y., Prenant, C., Benavides, J., Scatton, B., Crouzel, C., Hauw, J. J., and Syrota, A. (1991) Pet Study of Carbon-11-Pk 11195 Binding to Peripheral Type Benzodiazepine Sites in Glioblastoma—a Case-Report. *J. Nucl. Med. 32*, 1608−1610.
(26) Miyazawa, N., Hamel, E., and Diksic, M. (1998) Assessment of the peripheral benzodiazepine receptors in human gliomas by two methods. *J. Neuro-Oncol. 38*, 19−26.
(27) Banati, R. B., Newcombe, J., Gunn, R. N., Cagnin, A., Turkheimer, F., Heppner, F., Price, G., Wegner, F., Giovannoni, G., Miller, D. H., Perkin, G. D., Smith, T., Hewson, A. K., Bydder, G., Kreutzberg, G. W., Jones, T., Cuzner, M. L., and Myers, R. (2000) The peripheral benzodiazepine binding site in the brain in multiple sclerosis—Quantitative in vivo imaging of microglia as a measure of disease activity. *Brain 123*, 2321−2337.
(28) Wang, D. C., Fryer, T., Price, C., Cleij, M., Aigbirhio, F., Green, H., Clark, J., Menon, D., Warburton, L., and Baron, J. C. (2004) Effect of CBV correction on ischaemic stroke [11C]-PK11195 binding potential values produced using a simplified reference tissue model. *Neuroimage 22*, T96−T97.
(29) Kozikowski, A. P., Kotoula, M., Ma, D. W., Boujrad, N., Tuckmantel, W., and Papadopoulos, V. (1997) Synthesis and biology of a 7-nitro-2,1,3-benzoxadiazol-4-yl derivative of 2-phenylindole-3-acetamide: A fluorescent probe for the peripheral-type benzodiazepine receptor. *J. Med. Chem. 40*, 2435−2439.
(30) Shilova, N. V., and Bovin, N. V. (2003) Fluorescent labels for the analysis of mono- and oligosaccharides. *Russ. J. Bioorg. Chem. 29*, 309−324.
(31) Chen, Y., Zheng, X., Dobhal, M. P., Gryshuk, A., Morgan, J., Dougherty, T. J., Oseroff, A., and Pandey, R. K. (2005) Methyl pyropheophorbide-a analogues: Potential fluorescent probes for the peripheral-type benzodiazepine receptor. Effect of central metal in photosensitizing efficacy. *J. Med. Chem. 48*, 3692−3695.
(32) Manning, H. C., Bai, M. F., Anderson, B. M., Lisiak, R., Samuelson, L. E., and Bornhop, D. J. (2005) Expeditious synthesis of 'P'-protected macrocycles en route to lanthanide chelate metal complexes. *Tetrahedron Lett. 46*, 4707−4710.
(33) Manning, H. C., Goebel, T., Marx, J. N., and Bornhop, D. J. (2002) Facile, efficient conjugation of a trifunctional lanthanide chelate to a peripheral benzodiazepine receptor ligand. *Org. Lett. 4*, 1075−1078.
(34) Manning, H. C., Goebel, T., Thompson, R. C., Price, R. R., Lee, H., and Bornhop, D. J. (2004) Targeted molecular imaging agents for cellular-scale bimodal imaging. *Bioconjugate Chem. 15*, 1488−1495.
(35) Okubo, T., Yoshikawa, R., Chaki, S., Okuyama, S., and Nakazato, A. (2004) Design, synthesis, and structure-activity relationships of novel tetracyclic compounds as peripheral benzodiazepine receptor ligands. *Bioorg. Med. Chem. 12*, 3569−3580.
(36) Munujos, P., Collcanti, J., Gonzalezsastre, F., and Gella, F. J. (1993) Assay of Succinate-Dehydrogenase Activity by a Colorimetric-Continuous Method Using Iodonitrotetrazolium Chloride as Electron-Acceptor. *Anal. Biochem. 212*, 506−509.
(37) Olson, J. M., Mcneel, W., Young, A. B., and Mancini, W. R. (1992) Localization of the Peripheral-Type Benzodiazepine Binding-Site to Mitochondria of Human Glioma-Cells. *J. Neuro-Oncol. 13*, 35−42.

BC060020B